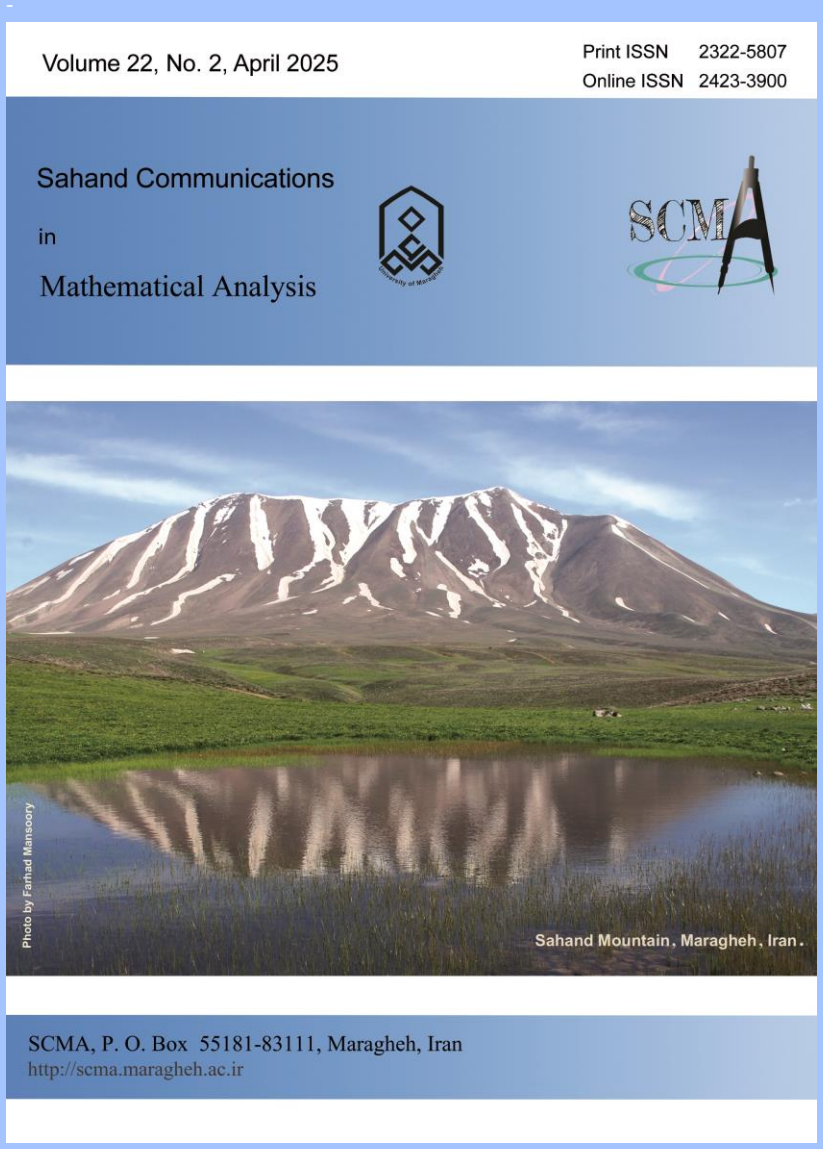
Analysis of Thermal Properties of Brain Tissues with Bioheat Transfer by Reduced Differential Transform Approach

Madhuri Sonje and Chandrashekhar Sutar

Sahand Communications in Mathematical Analysis

Print ISSN: 2322-5807
Online ISSN: 2423-3900
Volume: 22
Number: 2
Pages: 223-245

Sahand Commun. Math. Anal.
DOI: 10.22130/scma.2024.2028288.1717



Sahand Communications in Mathematical Analysis (SCMA) Vol. 22 No. 2 (2025), 223-245
http://scma.maragheh.ac.ir
DOI: 10.22130/scma.2024.2028288.1717

Analysis of Thermal Properties of Brain Tissues with Bioheat Transfer by Reduced Differential Transform Approach

Madhuri Sonje[1*] and Chandrashekhar Sutar[2]

Abstract. Microwave ablation (MWA) for brain tumours is a highly effective treatment for destroying brain tumour cells, where energy is delivered through devices to increase the temperature of brain tumour cells. The primary goal of microwave ablation is to increase the temperature of brain tissues, which kills tumour cells. Raising the temperature can destroy tumoural cancer cells, usually with minimal damage to healthy organs. This paper presents the modelling of heat transfer of healthy and tumoural brain tissues during MWA treatment by using single phase lag Penne's bioheat theory. A mathematical model describing this process during MWA treatment provides valuable insights into the thermal effects of this treatment. The reduced differential transform technique represents the analytical solution for the temperature of healthy and tumoural brain tissues. This paper deals with the comparison of temperature distribution between healthy and tumoural brain tissue during MWA treatment. The thermoelastic properties of healthy and tumoural brain tissues have been discussed and compared by using Python graphs. Also, thermal damage on healthy brain tissues has been represented graphically. This knowledge contributes to the safety and optimization of MWA treatment.

1. Introduction

Nowadays, hyperthermia therapies are acknowledged as cancer treatment methods. One technique for treating tumours is hyperthermia, in which energy is delivered via devices to raise the temperature of body tissue cells. A high temperature is applied to tissues of the body as

2020 *Mathematics Subject Classification.* 35Q79, 35K05.
Key words and phrases. Microwave ablation (MWA), Reduced differential transform method, Single phase lag (SPL), Thermal damage, Linear thermal stresses.
Received: 2024-05-06, Accepted: 2024-11-19.
* Corresponding author.

part of this form of cancer therapy. High temperatures can harm and destroy cancer cells, generally with little harm to healthy tissues. It has been discovered that preserving good tissue while healing sick tissue is a difficult part. As a result, researchers are working to adapt basic engineering concepts in the disciplines of biology and medicine to create thermal treatments for treating contaminated living tissues.

There are various types of hyperthermia treatments depending on the temperature, such as adjuvant hyperthermia, real hyperthermia and ablative hyperthermia. During adjuvant hyperthermia treatment, temperatures rise between 38°C and 41°C; this treatment is combined with additional therapies, including radiation therapy and chemotherapy, to improve favourable outcomes while minimizing negative effects. When temperatures rise between 43°C to 46°C during treatment, this hyperthermia is considered to be real hyperthermia. Without tissue necrosis, permanent cellular damage is achieved in this instance by applying electromagnetic fields for 40–60 minutes. Finally, when the temperature reaches 50°C – 100°C in a matter of minutes during the hyperthermia therapy, then this is considered to be an ablative hyperthermia that has completely necrotised the tissues. Different types of electromagnetic radiation, including radiofrequency (Radio Frequency Ablation, RFA), Microwave Ablation (MWA) acoustic waves, or laser energy, can be used to carry out thermo-ablative procedures [3].

Injecting various nanoparticles to carry out thermal ablation in the treatment of brain tumours using radiofrequency technology was suggested by Shao et al. [18]. In their research, they updated Penne's bioheat model and applied it to two separate locations of the living tissue region and the damaged tissue region [18]. In this model, we have considered cylindrical brain tissue whose radius R= 50 mm and height h = 140 mm [5]. Every tumour in the brain is unique, thus the treatment option must be determined based on the size and shape of the tumour. Here we are considering an approximately spherical tumour having a radius of 0.7 cm. In all cases of MWA treatment, the tumour has been located with an imaging guide through the use of Aloka 5500 transoperative ultrasound. In the tumour's centre, a thin antenna (calibre 14.5; MedWaves) was inserted. Until the temperature sensor in the antenna reached 80°C-100°C, energy had been delivered for 3–9 min with 45 W of power and in two or three distinct vectors. During MWA process, the measured temperature of the brain surface has been 33°C to 36°C. An electronic thermometer (sterile esophageal thermometer) has been incorporated to record this temperature reading. The thermometer has been positioned in the cortical region next to the tumour with a temperature sensor on its top [16].

A.K. Datta [4] introduces the approach of heat and mass transfer regarding biological context. American physician and clinical researcher Harry H. Pennes [14] first time developed a mathematical model of the bioheat equation. P. K. Gupta et al [6] has observed that during thermal therapy, probe shape, boundary conditions and internal heat source should not be the same and must be changed from organ to organ in the human body. R. Kumar et al [8] have introduced a dual phase lag bioheat transfer model in the context of memory-dependent derivative. A. Andreozzi et al [3] have discussed modified bioheat models in various hyperthermia treatments of cancer. Tehrani et al [20] have discussed the effects of the size and shape of tumours on microwave ablation treatment and solved bioheat equations by using the three-dimensional finite element method. M. Radmilovic-Radjenovi et al [15] have determined input power and ablation time for successive tumour treatment. R. Tiwari et al [21] developed a dual phase lag bioheat model under different thermal conditions and studied temperature, displacement, strain and stress for different thermal conditions.

A. S. Ramírez et al [16] discussed MWA treatment in brain and skull-based tumour surgery. M. M. Elwassif et al [5] have discussed the bioheat transfer model of deep brain stimulation and provided information on the thermal effects of DBS using by finite element model. F. Morin et al [11] presented Biomechanical modelling of brain soft tissues and described a new vessel-based brain-shift compensation model using intraoperative Doppler ultrasound imaging. I. Abbas et al [1] developed a two-dimensional single-phase-lag (SPL) bioheat transfer model in biological tissue by considering the heat conduction law and discussed the results graphically. H. M. Youssef [23] have developed a one-dimensional dual phase lag thermoelastic skin tissue model and solved it by using Laplace transformed and Tzuo method. Muhammad Amjad et al [2] discussed the Numerical study of heat and mass transfer for micropolar fluid flow due to two symmetrical stretchable disks. P. Shang et al [17] studied the effect of nanoparticle type on the fluid velocity component, temperature distribution, skin friction coefficient and Nusselt number.

In this paper, we presented a single-phase lag model that described the process of heat transfer in healthy and tumoural brain tissues separately during microwave ablation therapy. The reduced differential transform technique has been used to represent the analytical solution. The analytical solution obtained by reduced differential transform method (RDTM) is quite accurate and reliable than other traditional methods for solving any bioheat equation. Temperature distribution of healthy and tumoural tissues have been compared by using Python graphs. Also, different effects of thermal stresses, Displacement components and thermal

damages have been represented graphically. This information will help enhance the security and effectiveness of MWA therapy.

2. Reduced Differential Transform Method

The concept of the reduced differential transform method is derived from the power series expansion. If the function $T(r, z, t)$ is analytic and continuously differentiable w.r.t. time t and space in the domain of interest, then the reduced differential transform function of $T(r, z, t)$ is defined by [10, 19].

$$\tau_k(r, z, t) = \frac{1}{k!}\left[\frac{\partial^k}{\partial t^k}T(r, z, t)\right]_{t=0}.$$

The inverse reduced differential function of $\tau_k(r, z, t)$ is defined as follows.

$$T(r, z, t) = \sum_{k=0}^{\infty} \tau_k(r, z, t)t^k.$$

3. Mathematical Problem Formulation of Bioheat Transfer

Firstly, the American physician and clinical researcher Harry Pennes has developed a mathematical model of the bioheat equation given in 1948 [14].

$$\rho C_t \frac{\partial T}{\partial t} = k\nabla^2 T + Q - \omega_b C_b(T - T_a).$$

Here we have used microwave ablation (MWA) hyperthermia to treat brain tumours. The governing equation of heat flow in brain tissues during MWA hyperthermia treatment is studied by using a single phase lag (SPL) model of modified Penne's bioheat equation which is given by as follows[1].

$$\begin{aligned}\rho c_p\left(1 + \tau_q\frac{\partial}{\partial t}\right)\frac{\partial T}{\partial t} = k'\frac{\partial^2 T}{\partial r^2} + \frac{k'}{r}\frac{\partial T}{\partial r} + k'\frac{\partial^2 T}{\partial z^2} \\ + \rho_b\omega_b c_b\left(1 + \tau_q\frac{\partial}{\partial t}\right)(T_a - T) \\ + \left(1 + \tau_q\frac{\partial}{\partial t}\right)(Q_{met} + Q_{ext}).\end{aligned}$$

Heat is produced through dielectric hysteresis in microwave ablation. When tissues are heated to deadly temperatures by an applied electromagnetic field, which is generally at 900-2500 MHz, tissue damage takes place. The oscillating electric field forces tissue's polar molecules, mostly H_2O, to constantly realign, raising their kinetic energy and the tissue's

temperature as a result[9]. During this therapy brain tissue temperature rises highly, so evaporation has been adjusted by adding a factor for the energy required to vaporise water in Pennes bioheat equation. Then SPL model of Penne's bioheat equation becomes as follows.

$$\rho c_p \left(1+\tau_q \frac{\partial}{\partial t}\right)\frac{\partial T}{\partial t} = k'\frac{\partial^2 T}{\partial r^2} + \frac{k'}{r}\frac{\partial T}{\partial r} + k'\frac{\partial^2 T}{\partial z^2} + \rho_b \omega_b c_b \left(1+\tau_q \frac{\partial}{\partial t}\right)(T_a - T) + \left(1+\tau_q \frac{\partial}{\partial t}\right)(Q_{met}+Q_{ext}) + \left(1+\tau_q \frac{\partial}{\partial t}\right)Q_E,$$

where, τ_q = phase lag of heat flux density, ρ= density of brain tissue, c_p= specific heat of brain tissue, k'= thermal conductivity of brain tissue, c_b= specific heat of the blood, w_b= blood perfusion rate, p_b= blood mass density, $T(r,\theta)$= brain tissue temperature, T_a= arterial blood temperature, Q_{met} = metabolic heat source = 368.1Wm-3 [21], Q_{ext}= microwave power density, where

$$Q_{ext} = \frac{\rho'(E^2)}{2},$$

here ρ' = effective electric conductivity
and E = modulus of electric field
i.e. Q_{ext}= heat of the resistance produced by electromagnetic field [23], Q_E = amount of energy required to vaporize water.
The amount of energy required to vaporize tissue water i.e. Q_E is a temperature-dependent function in MWA hyperthermia treatment [3]. Here we have considered,

$$Q_E = \gamma\left(227.4853 exp\left(\frac{T-106}{3.42}\right)\frac{dT}{dt}\right),$$

where γ is the water latent heat constant = 2260 kJ kg-1 [3].
Temperature distribution of brain tissues during MWA treatment has been discussed by applying updated SPL Penne's bioheat model on two separate locations of healthy brain tissues and tumoural brain tissues region as follows.

Case I: Temperature distribution of healthy brain tissues
For healthy brain tissues, the governing equation of the SPL bioheat transfer model is

(3.1)

$$\rho c_p \left(1+\tau_q \frac{\partial}{\partial t}\right)\frac{\partial T}{\partial t} = k'\frac{\partial^2 T}{\partial r^2} + \frac{k'}{r}\frac{\partial T}{\partial r} + k'\frac{\partial^2 T}{\partial z^2}$$

$$+\rho_b\omega_b c_b\left(1+\tau_q\frac{\partial}{\partial t}\right)(T_a-T)$$
$$+\left(1+\tau_q\frac{\partial}{\partial t}\right)(Q_{met}+Q_{ext})$$
$$+\left(1+\tau_q\frac{\partial}{\partial t}\right)\gamma\left(227.4853exp\left(\frac{T-106}{3.42}\right)\frac{dT}{dt}\right).$$

With initial and boundary conditions given by

$$T(r,z,0)=T_0, r=R, \tag{3.2}$$
$$T_a(r,z,0)=T_1, \tag{3.3}$$
$$\frac{\partial T(r,z,0)}{\partial t}=0, \tag{3.4}$$
$$\frac{\partial T_a(r,z,0)}{\partial t}=0. \tag{3.5}$$

In this model, we have considered cylindrical brain tissue whose radius R= 50 mm and height h = 140 mm [5].

Considering,

$$T_0=\sum_{m=1}^{\infty}\sum_{n=1}^{\infty}C_{mn}\sin\left(\frac{m\pi r}{R}\right)\sin\left(\frac{n\pi z}{h}\right),$$

where $0\le r\le R$ & $0\le z\le h$.

The generalized solution to the problem has been obtained by using the reduced differential transform method [10, 19].

After applying RDTM on (3.1) to (3.5), we get a generalized solution in two different forms for even and odd integers as follows:

i. If k is even, then

$$\tau_k(r,z,t)=\frac{1}{k!\rho^{\frac{k}{2}}c_p^{\frac{k}{2}}\tau_q^{\frac{k}{2}}}A_k, \tag{3.6}$$

where,

$$\begin{aligned}A_k &= k'(A_{k-2})_{rr}+\frac{k'}{r}(A_{k-2})_r+k'(A_{k-2})_{zz}\\ &+\rho_b\omega_b c_b\left(\frac{k}{2}\rho^{\frac{k}{2}-1}c_p^{\frac{k}{2}-1}\tau_q^{\frac{k}{2}-1}B_{k-2}-A_{k-2}\right)\\ &+\rho_b\omega_b c_b\tau_q\left((k-1)!\rho^{\frac{k}{2}-1}c_p^{\frac{k}{2}-1}\tau_q^{\frac{k}{2}-1}B_{k-1}-A_{k-1}\right)-\rho c_p A_{k-1}\\ &+(k-2)!\rho^{\frac{k}{2}-1}c_p^{\frac{k}{2}-1}\tau_q^{\frac{k}{2}-1}\left((Q_{met})_{k-2}+(Q_{ext})_{k-2}+(Q_E)_{k-2}\right)\end{aligned} \tag{3.7}$$

$$+ (k-2)!\rho^{\frac{k}{2}-1}c_p^{\frac{k}{2}-1}\tau_q^{\frac{k}{2}}\left((Q_{met})_{k-1} + (Q_{ext})_{k-1} + (Q_E)_{k-1}\right).$$

After applying inverse RDT on equation (3.6), we get

$$T(r,z,t) = \sum_{k=0}^{\infty} \tau_k t^k.$$

$$\therefore T(r,z,t) = A_0 + \sum_{k=1}^{\infty} \frac{1}{k!\rho^{\frac{k}{2}}c_p^{\frac{k}{2}}\tau_q^{\frac{k}{2}}} A_k t^k,$$

where
$A_0 = T(r,z,0)$.

ii. If k is odd, then

$$\tau_k = \frac{1}{k!\rho^{\frac{k+1}{2}-1}c_p^{\frac{k+1}{2}-1}\tau_q^{\frac{k+1}{2}-1}} A_k, \tag{3.8}$$

where,

$$\begin{aligned} A_k = {} & k'(A_{k-2})_{rr} + \frac{k'}{r}(A_{k-2})_r + k'(A_{k-2})_{zz} - \frac{A_{n-1}}{\tau_q} \\ & + \rho_b\omega_b c_b\left((k-2)!\rho^{\frac{k+1}{2}-2}c_p^{\frac{k+1}{2}-2}\tau_q^{\frac{k+1}{2}-2}B_{k-2} - A_{k-2}\right) \\ & + \rho_b\omega_b c_b\tau_q\left((k-1)!\rho^{\frac{k+1}{2}-2}c_p^{\frac{k+1}{2}-2}\tau_q^{\frac{k+1}{2}-2}B_{k-1} - A_{k-1}\right) \\ & + (k-2)!\rho^{\frac{k+1}{2}-2}c_p^{\frac{k+1}{2}-2}\tau_q^{\frac{k+1}{2}-2}\left((Q_{met})_{k-2} + (Q_{ext})_{k-2} + (Q_E)_{k-2}\right) \\ & + (k-2)!\rho^{\frac{k+1}{2}-2}c_p^{\frac{k+1}{2}-2}\tau_q^{\frac{k+1}{2}-2}\left((Q_{met})_{k-1} + (Q_{ext})_{k-1} + (Q_E)_{k-1}\right). \end{aligned}$$

After applying inverse RDT on equation (3.8), we get

$$T(r,z,t) = \sum_{k=0}^{\infty} \tau_k t^k.$$

$$\therefore T(r,z,t) = A_0 + \sum_{k=1}^{\infty} \frac{1}{k!\rho^{\frac{k+1}{2}-1}c_p^{\frac{k+1}{2}-1}\tau_q^{\frac{k+1}{2}-1}} A_k t^k,$$

where $A_0 = T(r,z,0)$.

Case II: Temperature distribution of tumoural brain tissues

For tumoural brain tissues, both blood perfusion rate ω_b and metabolic heat Q_{met} are zero [18].

Hence, the governing equation of the SPL bioheat transfer model is

$$\rho c_p\left(1+\tau_q\frac{\partial}{\partial t}\right)\frac{\partial T}{\partial t}=k'\frac{\partial^2 T}{\partial r^2}+\frac{k'}{r}\frac{\partial T}{\partial r}+k'\frac{\partial^2 T}{\partial z^2}+\left(1+\tau_q\frac{\partial}{\partial t}\right)Q_{ext}+\left(1+\tau_q\frac{\partial}{\partial t}\right)\gamma\times\left(227.4853exp\left(\frac{T-106}{3.42}\right)\frac{dT}{dt}\right). \tag{3.9}$$

With same initial and boundary conditions as per healthy tissues given by

$$T(r,z,0)=T_0, r=R, \tag{3.10}$$

$$T_a(r,z,0)=T_1, \tag{3.11}$$

$$\frac{\partial T(r,z,0)}{\partial t}=0, \tag{3.12}$$

$$\frac{\partial T_a(r,z,0)}{\partial t}=0. \tag{3.13}$$

Considering,

$$T_0=\sum_{m=1}^{\infty}\sum_{n=1}^{\infty}C_{mn}\sin\left(\frac{m\pi r}{R}\right)\sin\left(\frac{n\pi z}{h}\right),$$

where $0\le r\le R$ & $0\le z\le h$.

The generalized solution of the problem has been obtained by using the reduced differential transform method [10, 19].

After applying RDTM on (3.9) to (3.13), we get a generalized solution in two different forms for even and odd integers as follows:

i. If k is even, then

$$\tau_k=\frac{1}{k!\rho^{\frac{k}{2}}c_p^{\frac{k}{2}}\tau_q^{\frac{k}{2}}}A_k, \tag{3.14}$$

where,

$$A_k=k'\left(A_{k-2}\right)_{rr}+\frac{k'}{r}\left(A_{k-2}\right)_r+k'\left(A_{k-2}\right)_{zz}-\rho c_p A_{k-1}+(k-2)!\rho^{\frac{k}{2}-1}c_p^{\frac{k}{2}-1}\tau_q^{\frac{k}{2}-1}\left((Q_{ext})_{k-2}+(Q_E)_{k-2}\right)+(k-2)!\rho^{\frac{k}{2}-1}c_p^{\frac{k}{2}-1}\tau_q^{\frac{k}{2}}\left((Q_{ext})_{k-1}+(Q_E)_{k-1}\right).$$

After applying inverse RDT on equation (3.14), we get

$$T(r,z,t)=\sum_{k=0}^{\infty}\tau_k t^k.$$

$$\therefore T(r,z,t) = A_0 + \sum_{k=1}^{\infty} \frac{1}{k!\rho^{\frac{k}{2}} c_p^{\frac{k}{2}} \tau_q^{\frac{k}{2}}} A_k t^k,$$

where $A_0 = T(r,z,0)$.

ii. If k is odd, then

$$\tau_k = \frac{1}{k!\rho^{\frac{k+1}{2}-1} c_p^{\frac{k+1}{2}-1} \tau_q^{\frac{k+1}{2}-1}} A_k, \tag{3.15}$$

where,

$$\begin{aligned} A_k = {} & k' \left(A_{k-2}\right)_{rr} + \frac{k'}{r} \left(A_{k-2}\right)_r + k' \left(A_{k-2}\right)_{zz} - \frac{A_{n-1}}{\tau_q} \\ & + (k-2)!\rho^{\frac{k+1}{2}-2} c_p^{\frac{k+1}{2}-2} \tau_q^{\frac{k+1}{2}-2} \left((Q_{ext})_{k-2} + (Q_E)_{k-2}\right) \\ & + (k-2)!\rho^{\frac{k+1}{2}-2} c_p^{\frac{k+1}{2}-2} \tau_q^{\frac{k+1}{2}-2} \left((Q_{ext})_{k-1} + (Q_E)_{k-1}\right). \end{aligned}$$

After applying inverse RDT on equation (3.15), we get

$$T(r,z,t) = \sum_{k=0}^{\infty} \tau_k t^k.$$

$$\therefore T(r,z,t) = A_0 + \sum_{k=1}^{\infty} \frac{1}{k!\rho^{\frac{k+1}{2}-1} c_p^{\frac{k+1}{2}-1} \tau_q^{\frac{k+1}{2}-1}} A_k t^k,$$

where $A_0 = T(r,z,0)$.

4. Thermal Properties of Brain Tissues During MWA treatment

4.1. **Thermal Stresses on Brain Tissues.** Brain tissue temperature rises during MWA treatment of brain tumours, which causes linear thermal stresses on brain tissue. These linear thermal stresses have been calculated using the following equations [13].

$$\begin{aligned} \sigma_{rr} &= 2\mu \left(\frac{\partial^2 \phi}{\partial r^2} - k_1 T(r,z,t) + \frac{\partial^2 \vartheta}{\partial r^2} + z \frac{\partial^2 \psi}{\partial r^2} - 2v \frac{\partial \psi}{\partial z} \right), \\ \sigma_{zr} &= 2\mu \left(\frac{\partial^2 \phi}{\partial z \partial r} + \frac{\partial^2 \vartheta}{\partial z \partial r} + z \frac{\partial^2 \psi}{\partial z \partial r} - (1-2v) \frac{\partial \psi}{\partial r} \right), \\ \sigma_{zz} &= 2\mu \left(\frac{\partial^2 \phi}{\partial z^2} - k_1 T(r,z,t) + \frac{\partial^2 \vartheta}{\partial z^2} + z \frac{\partial^2 \psi}{\partial z^2} - 2(1-v) \frac{\partial \psi}{\partial z} \right). \end{aligned}$$

Here the function ϕ is Goodier's thermoelastic displacement function which satisfies equation [13].

$$\nabla^2 \phi = k_1 (T - T_0), \tag{4.1}$$

with boundary conditions, $\phi(r,0) = -r^4$ and $\phi'(r,0) = D_0$ and ψ and ϑ are Boussinesq harmonic functions must satisfy the equations [13].

$$\nabla^2\psi = 0, \tag{4.2}$$

with boundary conditions, $\psi(r,0) = r^2$ and $\psi'(r,0) = A_0$ and,

$$\nabla^2\vartheta = 0, \tag{4.3}$$

with boundary conditions, $\vartheta(r,0) = r^3$ and $\vartheta'(r,0) = B_0$.

After applying reduced differential transform method on equation (4.1),(4.2),(4.3), then we get

$$\phi = r^4 + D_0 z + 8r^2z^2 + \frac{k_1}{6}\tau_1 z^3 + \cdots \tag{4.4}$$

$$\psi = r^2 + A_0 z - 2z^2 + 0. \tag{4.5}$$

$$\vartheta = r^3 + B_0 z - \frac{9}{2}rz^2 + 0z^3 + \frac{3}{8}\frac{1}{r}z^4 + \cdots \tag{4.6}$$

Thus linear thermal stresses on brain tissues during microwave ablation treatment are

$$\sigma_{rr} = 2\mu\left(12r^2 + 16z^2 + \frac{k_1}{6}z^3 - k_1\tau + 6r + \frac{3}{4r^3}z^4 + 2z - 2v(A_0 - 4z)\right),$$

$$\sigma_{zz} = 2\mu\left(16r^2 - k_1\tau - 9r + \frac{9}{2r}z^2 - 4z - 2(1-v)(A_0 - 4z)\right),$$

$$\sigma_{zr} = 2\mu\left(32rz - 9z + \frac{3}{2}z^3 - (1-2v)2r\right),$$

where ϑ_1 is the Poisson ratio of brain tissues = 0.45 [8], α is coefficient of linear thermal expansion = 0.00015[17], E is Young's modulus = 2.1 kPa [11],

$$\mu = \frac{E}{2(1+\vartheta_1)} = 0.7242,$$

$$k_1 = \left(\frac{1+\vartheta_1}{1-\vartheta_1}\right)\alpha = 0.000395466.$$

4.2. **Thermoelastic Displacement Components.** The thermoelastic displacement functions are given by [13]

$$u_r = \frac{\partial\phi}{\partial r} + \frac{\partial\vartheta}{\partial r} + z\frac{\partial\psi}{\partial r}. \tag{4.7}$$

and

$$u_z = \frac{\partial\phi}{\partial z} + \frac{\partial\vartheta}{\partial z} + z\frac{\partial\psi}{\partial z} - (3-4v)\psi. \tag{4.8}$$

Using equations(4.4),(4.5),(4.6) in (4.7) & (4.8) we get,

$$u_r = \left(4r^3 + 3r^2 + 2rz + \left(16r - \frac{9}{2}\right) z^2 + \frac{k_1}{6} (\tau_1)_r z^3 - \frac{3}{8r^2} z^4 + \cdots \right).$$

$$u_z = B_0 + D_0 + (-9r + 16r^2)z + A_0 + \frac{k_1}{2}\tau_1 z^2 - 4z^2 + \frac{3}{2r} z^3 - (3 - 4v)(r^2 + A_0 z - 2z^2).$$

5. Thermal Damage of Brain Tissues

Optimal microwave ablation treatment time for brain tumours depends on the shape and size of the tumour. Extra treatment time affects normal brain tissues and causes thermal damage to normal tissues. Also, if brain temperature increases above a certain value then thermal damages are generated during MWA therapy. The Arrhenius burn integration has been developed by Henriques and Moritz [7, 12] and is widely used by many researchers. According to their claims, skin damage is described as a chemical rate process that has been quantified using a first-order Arrhenius rate equation.

Thermal damage of brain tissues has been determined by using the Arrhenius integral formula.

$$\omega = \int_0^t B exp\left(\frac{-E_a}{ST}\right) dt,$$

where $B = 5.0 \times 10^{45} s^{-1}$ is frequency factor, $E_a = 2.96 \times 10^5$J/mol is activation energy, and $S = 8.314 J/mol$ is universal gas constant [22].

6. Graphical Results

In the current section, we have derived the nature of the temperature distributions of brain tissues which have been represented through the graphical results obtained by using Python. Tissue Properties are as follows [23]

Tissue Properties	**Symbol**	**Value**	**Unit**
Brain tissue density	ρ	1079	kg/m^3
Specific heat of the brain tissue	C_p	3540	$J/kg\,^\circ C$
Thermal conductivity of brain tissue	k'	0.52	$W/m\,^\circ C$
Initial temperature of brain tissue	T_0	37	$^\circ C$
Body core temperature	T_a	37	$^\circ C$
Poisson ratio of brain tissues	ϑ_1	0.45	Unitless
Coefficient of linear thermal expansion	α	0.00015	c^{-1}
Young's modulus	E	2.1	kPa
Blood Properties	**Symbol**	**Value**	**Unit**
Blood density	ρ_b	1055	kg/m^3
Blood perfusion rate	ω_b	0.005	$/s$
Specific heat of the blood	c_b	3600	$J/kg\,^\circ C$
tumour Properties	**Symbol**	**Value**	**Unit**
Density of the tumour	ρ_{tumour}	1040	kg/m^3
Specific heat of the tumour	C_{tumour}	3960	$J/kg\,^\circ C$
Thermal conductivity of the tumour	k'_{tumour}	0.57	$W/m\,^\circ C$

Analysis of Temperature Distribution of Brain Tissues During MWA Treatment

The temperature distributions of healthy and tumoural brain tissues have been discussed and represented by using Python graphs.

Fig 1 and Fig 2 show the temperature distribution of healthy tissues and tumoural tissues respectively w.r.t. time t. It shows that as time increases temperature of brain tissues also increases i.e. temperature is directly proportional to time. From Fig 1 and Fig 2 we conclude that the temperature of healthy tissues is greater than the temperature of tumoural tissues during MWA treatment but the nature of both curves is the same.

Fig 3 and Fig 4 show the temperature distribution of healthy tissues and tumoural tissues respectively w.r.t. radial distance of brain tissue r. It shows that the nature of both graphs is the same and in both cases initially, the temperature is greater but it decreases up to r = 25 (i.e. at the middle value of the radius of brain tissues) and after that, it increases. Figures show the curves for four different timings. Again here we conclude that the temperature of healthy tissues is slightly greater than the temperature of tumoural tissues during MWA treatment.

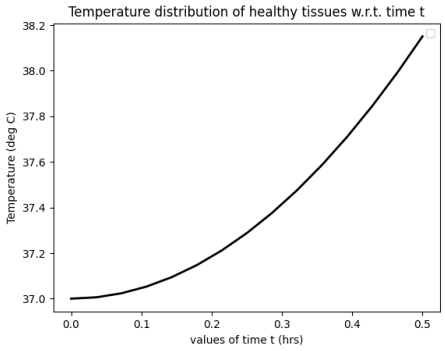


FIGURE 1. T for healthy tissues w.r.t. time t

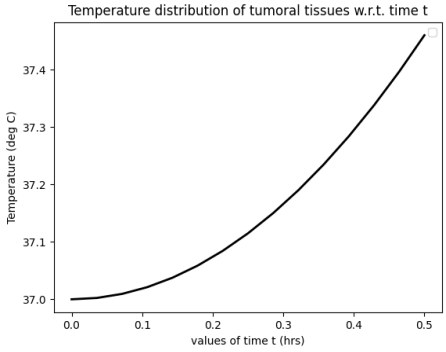


FIGURE 2. T for tumoural tissues w.r.t. time t

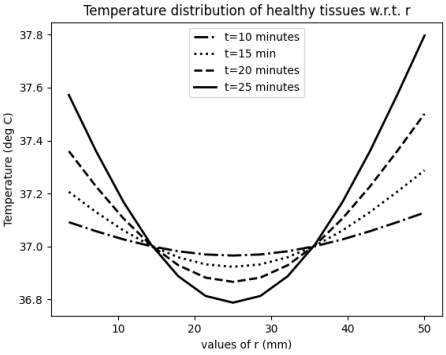


FIGURE 3. T for healthy tissues w.r.t.'r'

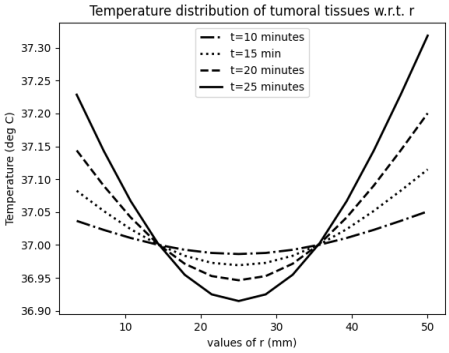


FIGURE 4. T for tumoural tissues w.r.t.'r'

Fig 5 and Fig 6 show the temperature distribution of healthy tissues and tumoural tissues respectively w.r.t. thickness of brain tissue z. It indicates that the nature of both graphs are same and in both cases, the temperature is constant w.r.t. z. Figures show the curves for four different timings. Again here we conclude that the temperature of healthy tissues is slightly greater than the temperature of tumoural tissues during MWA treatment.

Fig 7 and Fig 8 show thermal stresses σ_{rr} on healthy and tumoural brain tissues respectively during MWA treatment w.r.t. r for four different locations. The graph indicates that initially i.e. near to brain surface thermal stresses are high during MWA treatment after that they

decrease rapidly up to approximately r = 15 and then thermal stresses are constant. From Fig 7 and Fig 8 we conclude that thermal stresses are the same on healthy and tumoural tissues.

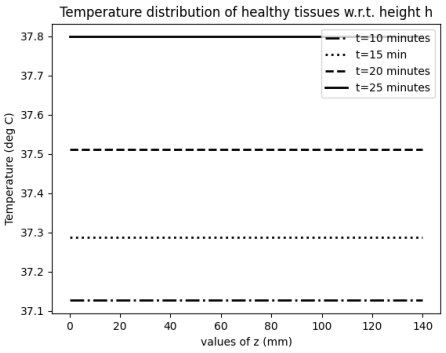


FIGURE 5. T for healthy tissues w.r.t. z

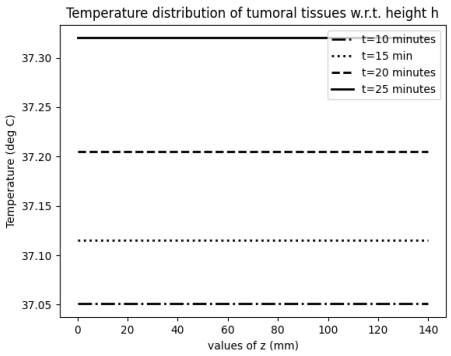


FIGURE 6. T for tumoural tissues w.r.t. z

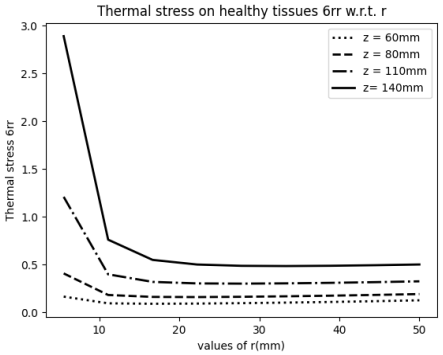


FIGURE 7. σ_{rr} on healthy tissues w.r.t. r

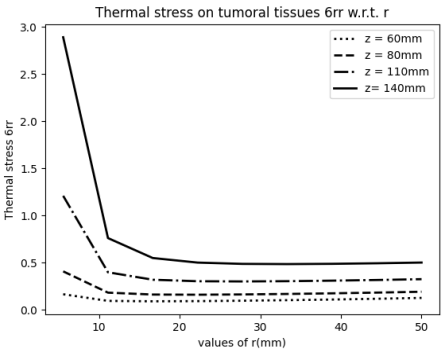


FIGURE 8. σ_{rr} on tumoural tissues w.r.t. r

Fig 9 and Fig 10 show thermal stresses σ_{rr} on healthy and tumoural brain tissues respectively during MWA treatment w.r.t. thickness z for four different values of r. The graph indicates that thermal stresses σ_{rr} increases exponentially as z increases. From four different curves of r, we conclude that stress is high for r =10 i.e. near to brain surface thermal stresses are high during MWA treatment.

Fig 11 and Fig 12 show thermal stresses σ_{rr} on healthy and tumoural brain tissues respectively during MWA treatment w.r.t. time t for four

different values of z. The graph indicates that thermal stresses σ_{rr} are constant w.r.t. time but stresses increase as z increases.

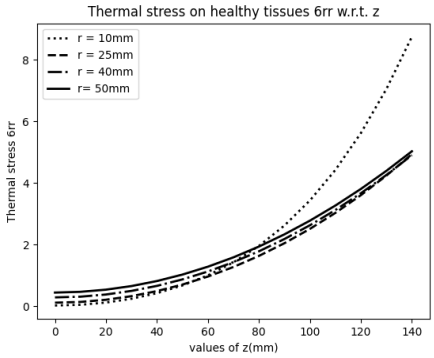


FIGURE 9. σ_{rr} on healthy tissues w.r.t. z

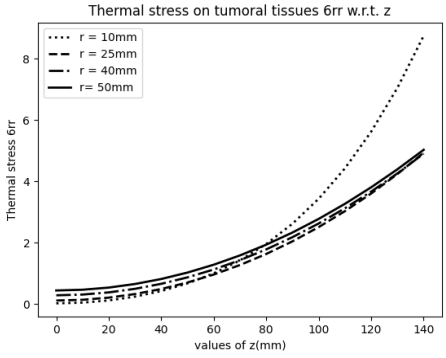


FIGURE 10. σ_{rr} on tumoural tissues w.r.t. z

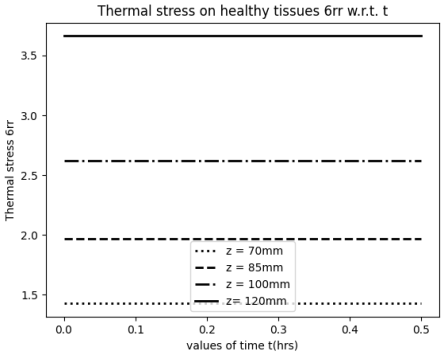


FIGURE 11. σ_{rr} on healthy tissues w.r.t.t

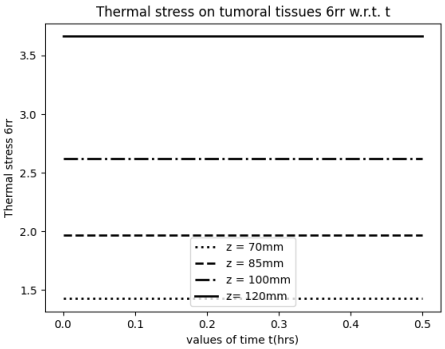


FIGURE 12. σ_{rr} on tumoural tissues w.r.t. t

Fig 13 and Fig 14 show thermal stresses σ_{zz} on healthy and tumoural brain tissues respectively during MWA treatment w.r.t. radial distance r for four different values of z. The graph indicates that initially thermal stresses σ_{zz} decrease up to approximately r = 12 but after that thermal stresses σ_{zz} increase rapidly.

Fig 15 and Fig 16 show thermal stresses σ_{zz} on healthy and tumoural brain tissues respectively during MWA treatment w.r.t. thickness z for four different values of r. The graph indicates that thermal stresses σ_{zz} increases slightly.

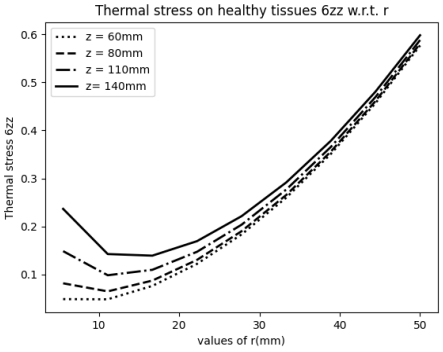


FIGURE 13. σ_{zz} on healthy tissues w.r.t. r

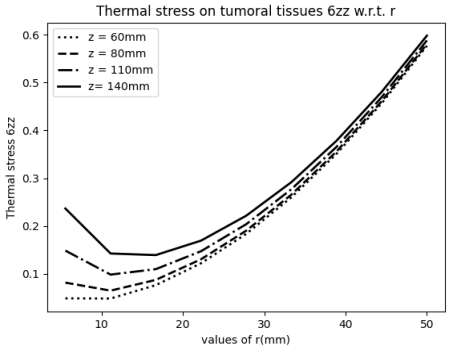


FIGURE 14. σ_{zz} on tumoural tissues w.r.t. r

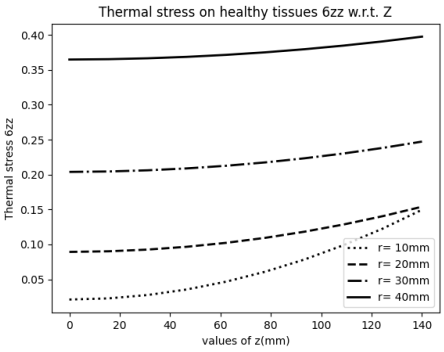


FIGURE 15. σ_{zz} on healthy tissues w.r.t. z

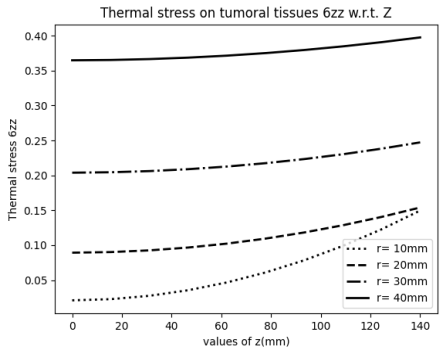


FIGURE 16. σ_{zz} on tumoural tissues w.r.t. z

Fig 17 and Fig 18 show thermal stresses σ_{zz} on healthy and tumoural brain tissues respectively during MWA treatment w.r.t. time t for four different values of z. The graph indicates that thermal stresses σ_{zz} are constant w.r.t. time but stresses increase as z increases.

Fig 19 and Fig 20 show thermal stresses σ_{zr} on healthy and tumoural brain tissues respectively during MWA treatment w.r.t. r for four different values of z. The graph indicates that thermal stresses σ_{zr} are increases rapidly as r increases.

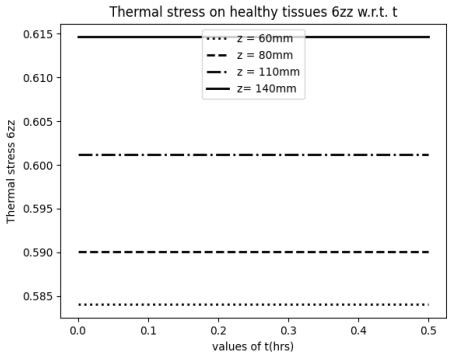


FIGURE 17. σ_{zz} on healthy tissues w.r.t. t

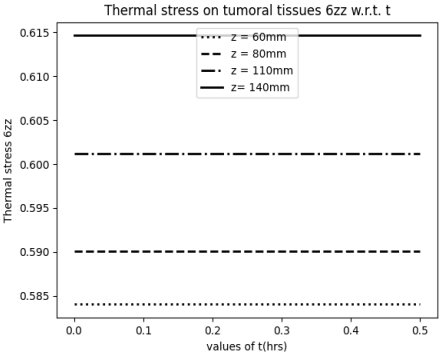


FIGURE 18. σ_{zz} on tumoural tissues w.r.t. t

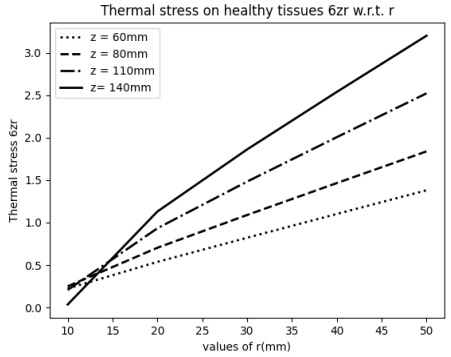


FIGURE 19. σ_{zr} on healthy tissues w.r.t. r

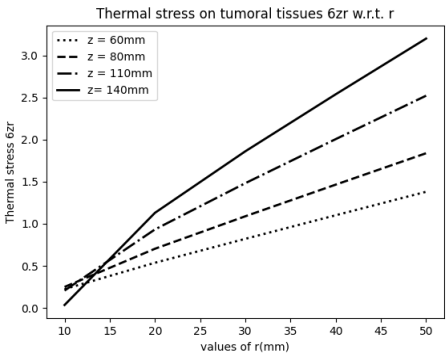


FIGURE 20. σ_{zr} on tumoural tissues w.r.t. r

Fig 21 and Fig 22 show thermal stresses σ_{zr} on healthy and tumoural brain tissues respectively during MWA treatment w.r.t. thickness z for four different values of r. The graph indicates that thermal stresses σ_{zr} increase rapidly as r increases and we conclude that thermal stresses σ_{zr} are directly proportional to the thickness of brain tissues z.

Fig 23 and Fig 24 show displacement component u_r w..r.t r and z respectively. In both cases displacement component u_r increases rapidly. From Fig 23 u_z increases linearly w.r.t. r and from Fig 24 u_z increases exponentially w.r.t. z.

Fig 25 and Fig 26 show displacement component u_z w..r.t r and z respectively. In both cases, displacement increases rapidly. From Fig 25

u_z increases exponentially w.r.t. r and from Fig 26 u_z increases linearly w.r.t. z.

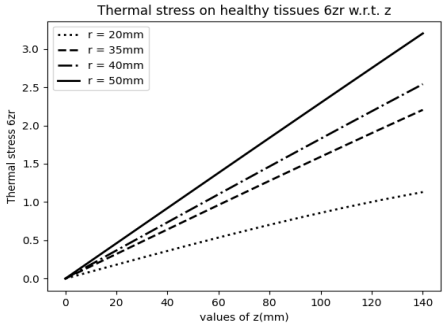


FIGURE 21. σ_{zr} on healthy tissues w.r.t. z

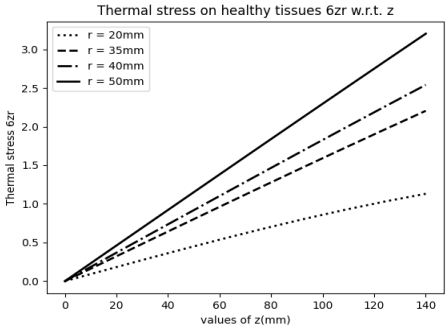


FIGURE 22. σ_{zr} on tumoural tissues w.r.t. z

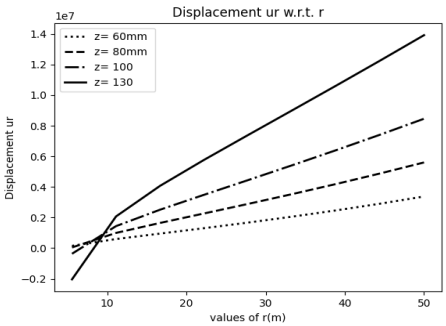


FIGURE 23. u_r w.r.t. r

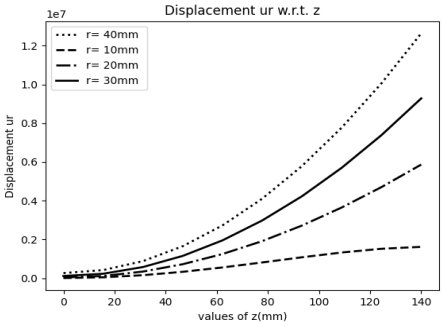


FIGURE 24. u_r w.r.t. z

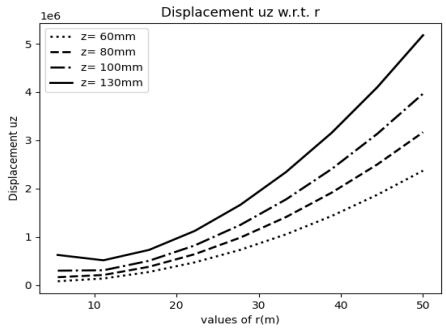


FIGURE 25. u_z w.r.t. r

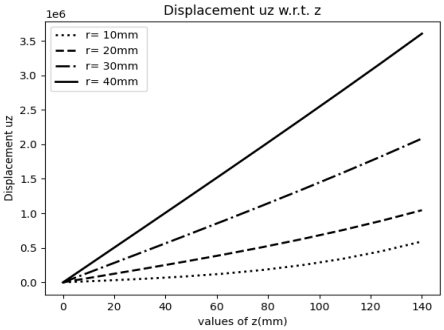


FIGURE 26. u_z w.r.t. z

Fig 27 represents the thermal damage of brain tissues w.r.t. time which indicates that thermal damage of brain tissues increases as the time of MWA treatment increases. Here we conclude that thermal damage of tissues depends on the period of therapy.

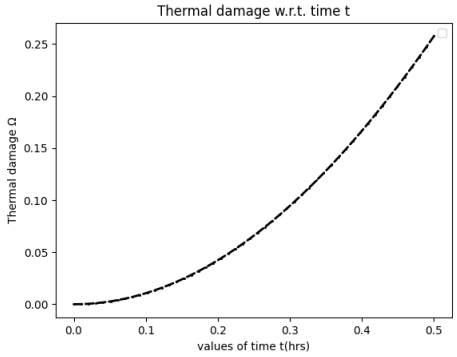


FIGURE 27. Thermal damage w.r.t.time t

Fig 28 and Fig 29 represent the thermal damage of brain tissues w.r.t. r and z respectively which show the thermal damage of brain tissues after half an hour of MWA treatment which lies between 0.2 to 0.3. Here we conclude that there is a slight change of thermal damage w.r.t. r and z means thermal damage does not more depends on r and z.

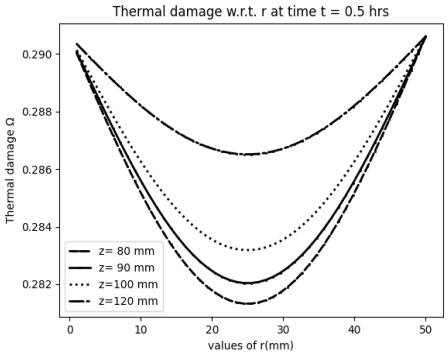


FIGURE 28. Thermal damage w.r.t. r

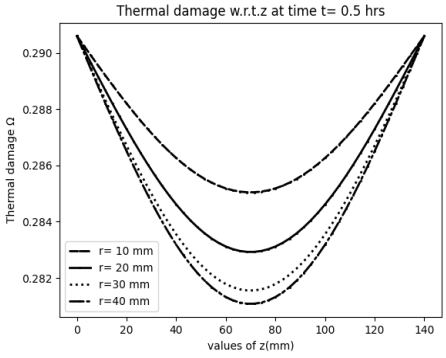


FIGURE 29. Thermal damage w.r.t. z

Fig 30 and Fig 31 represent the thermal damage of brain tissues w.r.t. r and z respectively for four different timings during MWA treatment. It indicates that there is a slight change in thermal damage w.r.t. r and z

but we have got four different curves for four different timings. Here we conclude that thermal damage of brain tissues depends on the time of MWA treatment and does not more depends on the radius and thickness of brain tissues.

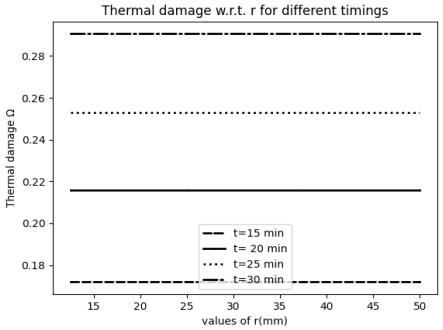


FIGURE 30. Thermal damage for different timings w.r.t. r

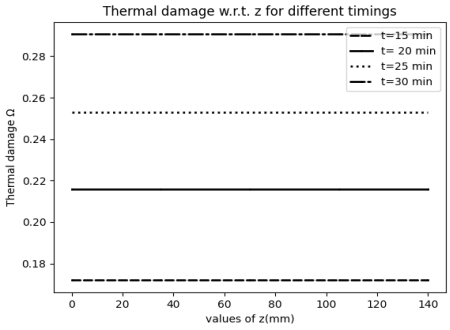


FIGURE 31. Thermal damage for different timings w.r.t. z

7. Conclusions

In the current paper, we have derived the mathematical model describing the process of heat transfer for healthy and tumoural brain tissues during MWA therapy. In this two-dimensional unsteady mathematical model, we have used a cylindrical coordinate system under different boundary conditions. The boundary value problem governing this process has been solved by using the reduced differential transform method. Temperature distribution of healthy and tumoural brain tissues have been compared graphically. Thermal damage of healthy brain tissues during MWA treatment is represented graphically. Also, linear thermal stresses and displacement components have been calculated by using the reduced differential transformed method and its different effects have been represented and studied by using Python graphs. Compared to other traditional methods, the analytical solution for the bioheat equation provided by the reduced differential transformation method (RDTM) is quite accurate and reliable than other traditional methods.

The following conclusions can be drawn from the graphical results.

1. The temperature of healthy tissues is slightly greater than the temperature of tumoural tissues during MWA treatment.

2. Linear thermal stresses on healthy and tumoural brain tissues are the same during MWA treatment.
3. Thermal damage of brain tissues depends on the period of MWA treatment and does not depend on the radius and thickness of tissue.

This information on temperature distribution and thermal properties of brain tissues obtained in the current study will be useful for preserving healthy tissues while healing tumoural tissue during thermal treatment. In the future, we will develop a fractional model of brain tissues during MWA treatment under sinusoidal heating and compare the results with the present analysis.

References

1. I. Abbas, A. Abdalla, F. Anwar and H. Sapoor, *A numerical solution of 2-D single-phase-lag (SPL) bioheat model using alternating direction implicit (ADI) finite difference method*, Sohag J. Sci., 7 (3) (2022), pp. 131-141.
2. M. Amjad, N. Ramzan, S. Ahmad, H. Ali, M. Alshehri and N.A. Shah, *Numerical study of heat and mass transfer for micropolar fluid flow due to two symmetrical stretchable disks*, Phys. Scr., 98 (10) (2023), p. 105227.
3. A. Andreozzi, L. Brunese, M. Iasiello, C. Tucci and G.P., *Modeling heat transfer in tumours: A review of thermal therapies*, Ann. Biomed. Eng., 47 (2019), pp. 676-693.
4. A.K. Datta, *Heat and Mass Transfer: A Biological Context*, CRC Press, Taylor and Francis Group, Boca Raton, London, New York, (2017).
5. M.M. Elwassif, Q. Kong, M. Vazquez and M. Bikson, *Bioheat transfer model of deep brain stimulation-induced temperature changes*, J. Neural Eng., 3 (4) (2006), p. 306.
6. P.K. Gupta, J. Singh and K.N. Rai, *A numerical study on heat transfer in tissues during hyperthermia*, Math. Comput. Model., 57 (5-6) (2013), pp. 1018-1037.
7. F.C. Henriques Jr. and A.R. Moritz, *Studies of thermal injury: I. The conduction of heat to and through skin and the temperatures attained therein*, Am. J. Pathol., 23 (4) (1947), p. 530.
8. R. Kumar, R. Tiwari, A. Singhal and S. Mondal, *Characterization of thermal damage of skin tissue subjected to moving heat source in the purview of dual-phase lag theory with memory-dependent derivative*, Waves Random Complex Media, (2021), pp. 1-18.

9. M.G. Lubner, C.L. Brace, J.L. Hinshaw and F.T. Lee Jr., *Microwave tumour ablation: mechanism of action, clinical results and devices*, J. Vasc. Interv. Radiol., 21 (8) (2010), pp. S192-S203.
10. M.S. Mohamed and K.A. Gepreel, *Reduced differential transform method for nonlinear integral member of Kadomtsev–Petviashvili hierarchy differential equations*, J. Egypt. Math. Soc., 25 (1) (2017), pp. 1-7.
11. F. Morin, M. Chabanas, H. Courtecuisse and Y. Payan, *Biomechanical modeling of brain soft tissues for medical applications*, in Biomechanics of Living Organs, Academic Press, (2017), pp. 127-146.
12. A.R. Moritz and F.C. Henriques Jr., *Studies of thermal injury: II. The relative importance of time and surface temperature in the causation of cutaneous burns*, Am. J. Pathol., 23 (5) (1947), p. 695.
13. N. Noda, R.B. Hetnarski and Y. Tanigawa, *Thermal Stresses*, second edition, Taylor and Francis Group, New York, London, (2003).
14. H.H. Pennes, *Analysis of tissue and arterial blood temperatures in the resting human forearm*, J. Appl. Physiol., 1 (2) (1948), pp. 93-122.
15. M. Radmilović-Radjenović, N. Bošković, M. Sabo and B. Radjenović, *An Analysis of Microwave Ablation Parameters for Treatment of Liver Tumours from the 3D-IRCADb-01 Database*, Biomedicines, 10 (7) (2022), p. 1569.
16. A.S. Ramírez, P.Á. Rodríguez, S.V.E. Gutiérrez and O.G. Ávila, *Preliminary experience in the management of brain and skull-base tumours with microwave ablation; feasibility guided by ultrasound, report from 23 cases*, Surg. Neurol. Int., 10 (2019).
17. P. Shang, A. Ali, H. Ali, M. Amjad, M. Ishaq and M.S. Aslam, *A comparative study of thermal performance of different nanofluids: An analytic approach*, Symmetry, 14 (11) (2022), p. 2439.
18. Y.L. Shao, B. Arjun, H.L. Leo and K.J. Chua, *Nano-assisted radiofrequency ablation of clinically extracted irregularly-shaped liver tumours*, J. Therm. Biol., 66 (2017), pp. 101-113.
19. V.K. Srivastava, M.K. Awasthi, R.K. Chaurasia and M. Tamsir, *The telegraph equation and its solution by reduced differential transform method*, Model. Simul. Eng., (2013), pp. 9-9.
20. M.H. Tehrani, M. Soltani, F.M. Kashkooli and K. Raahemifar, *Use of microwave ablation for thermal treatment of solid tumours with different shapes and sizes—A computational approach*, PLoS One, 15 (6) (2020), p. e0233219.
21. R. Tiwari, A. Singhal, R. Kumar, P. Kumar and S. Ghangas, *Investigation of memory influences on bioheat responses of skin tissue*

due to various thermal conditions, Theory Biosci., (2023), pp. 1-16.
22. F. Xu, P.F. Wang, M. Lin, T.J. Lu and E.Y.K. Ng, *Quantification and the underlying mechanism of skin thermal damage: a review*, J. Mech. Med. Biol., 10 (3) (2010), pp. 373-400.
23. H.M. Youssef and N.A. Alghamdi, *Modeling of one-dimensional thermoelastic dual-phase-lag skin tissue subjected to different types of thermal loading*, Sci. Rep., 10 (1) (2020), p. 3399.

---

[1] Department of First year Engineering Mathematics, Modern Education Society's Wadia College of Engineering, Pune 411 001, Maharashtra, India.

Email address: madhurimetkar09@gmail.com

[2] Department of Mathematics, PSGVPM's A.S.C. College, Shahada, Dist-Nandurbar 425 409 Maharashtra, India.

Email address: sutarchandu@gmail.com